Supporting Information

Novel chiral effect that produces the anisotropy in 3D structured soft material: chirality-driven cubic-tetragonal liquid crystal phase transition

Takahiro Yamamoto,[*a,b] Isa Nishiyama,[c] Makoto Yoneya[a,b] and Hiroshi Yokoyama[a,b]

[a] *Nanotechnology Research Institute, National Institute of Advanced Industrial Science and Technology, 1-1-1 Higashi, Tsukuba,305-8565, Japan. Fax: +81 29 861 6235; Tel: +81 29 861 3247; E-mail: takahiro.yamamoto@aist.go.jp*

[b] *Liquid-crystal Nano-system Project, ERATO/SORST, Japan Science and Technology Agency, 5-9-9 Tokodai, Tsukuba, 300-2635, Japan.*

[c] *Liquid Crystal Materials Technical Dept., DIC Corporation, 4472-1, Oaza Komuro, Ina-machi, Kita-Adachi-gun, Saitama, 362-8577, Japan*

1. Experimental details on XRD measurements: The X-ray scattering experiments were carried out by real-time X-ray diffractometer (Bruker AXS D8 Discover with GADDS). The monochromatic X-ray beam (CuK α line) was generated by 1.6 kW X-ray tube and Goebel mirror optics. The two-dimensional position sensitive detector has 1024 x 1024 pixels in a 5 cm x 5 cm beryllium window. A sample was introduced in a this glass capillary (diameter 1.0 mm), which was placed in a custom-made temperature stabilized holder (stability within $\pm 0.1\ ^{o}C$).

2. Structures of the SmQ phases

Figure S1 shows two-dimensional scattering patterns in the small angle region of two SmQ phases, denoted as SmQ_H and SmQ_L phases for the higher- and lower-temperature SmQ phases, respectively. The emergence of many diffraction spots indicates that both of the phases possess a 3D structure, rather than just a simple layered structure. Wide angle XRD patterns only show a broad scattering (figure S2), which means these SmQ phases possess a liquid-like short-range order, and thus are not higher-ordered smectic phases, such as SmB and SmE, or a real crystal phase. These results are consistent with the previous proposal that the SmQ_H and SmQ_L phases are liquid-crystalline 3D phases[1,2].

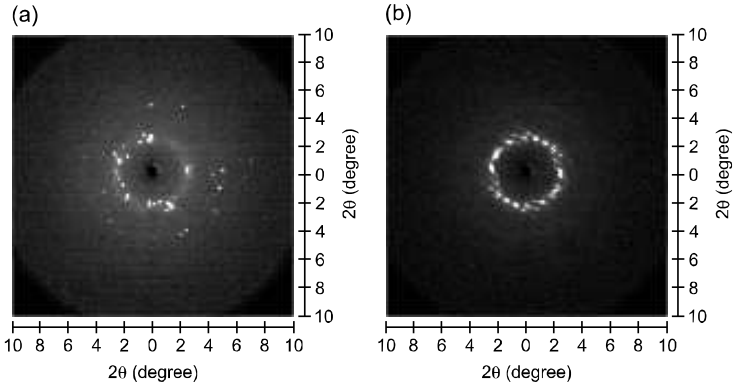

Figure S1 Two-dimensional X-ray scattering patterns in the small angle region: (a) SmQ_L and (b) SmQ_H

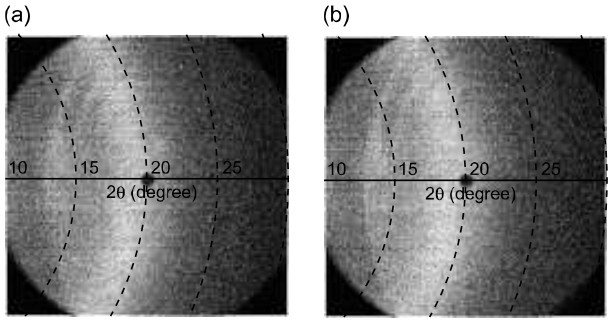

Figure S2 Two-dimensional X-ray scattering patterns in the wide angle region: (a) the SmQ_L phase and (b) SmQ_H phase.

The analysis of the scattering profile shows that the SmQ_H phase possesses a tetragonal structure, T*I, having a distinct space group of I422 with lattice constants of a = 63.1 Å and c = 65.5 Å (figure S3). This assignment is again consistent with the result of the miscibility test showing that the SmQ_H phase is miscible with the standard SmQ phase which had been found to have a tetragonal T*I structure[3]. Similarly, the SmQ_L phase is assigned as a tetragonal T*II phase, having a space group of $I4_122$, with lattice constants of a = 72.8 Å and c = 121.9 Å (figure S4). This assignment agrees with the polarized light microscope observation that the mosaic texture of the SmQ_L phase is similar to that reported for the tetragonal T*II phase[4,5]. The phase types, space groups, and lattice constants are summarized in Table 1.

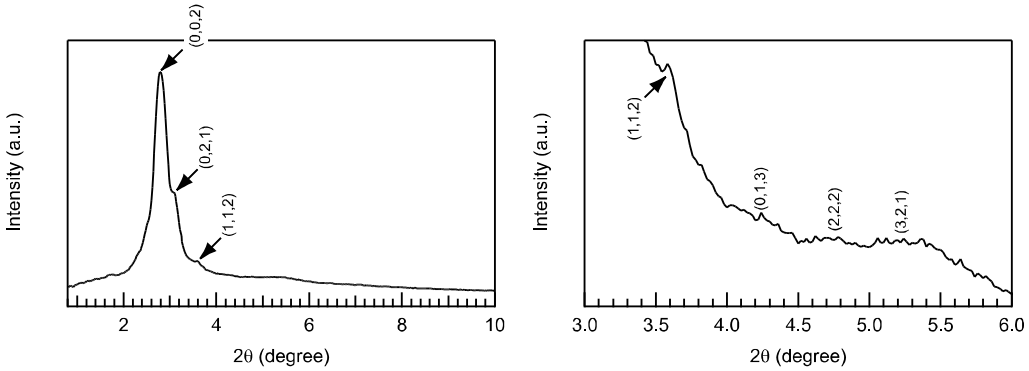

Figure S3 X-ray scattering profiles in the small angle region of the SmQ_H phase at 160 °C.

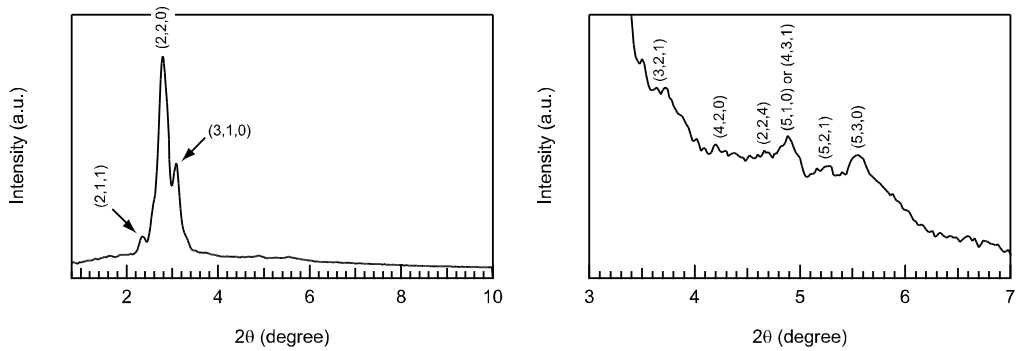

Figure S4 X-ray scattering profiles in the small angle region of the SmQ_L phase at 130 ^oC.

3. Structure of the cubic phase

Similar to the two-dimensional scattering patterns obtained for the SmQ phases, numerous and intense Bragg spots appear in the small angle region for the cubic phase, whereas just a broad scattering is observed in the wide angle region (figure S5). These XRD results indicate that the phase possesses a 3D structure with liquid-like short-range order, which is consistent with the assignment of the cubic phase. By indexing the Bragg spots, it was found that the cubic phase possesses a space group of Im3m (a = 78.3 Å) (figure S6). A similar structure is observed in the chiral cubic phase (figure S7, see the text for detailes).

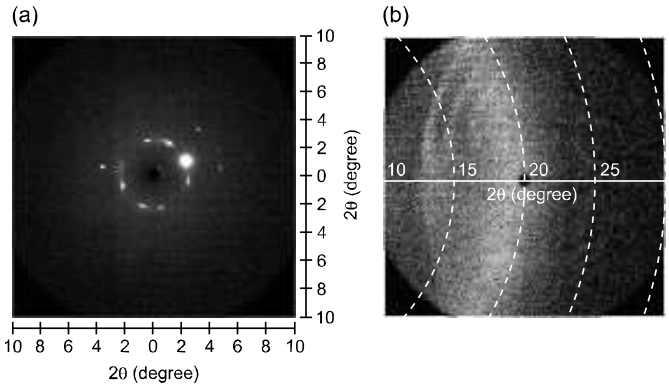

Figure S5 Two-dimensional X-ray scattering patterns observed in the racemic mixture: (a) in the small angle region and (b) in the wide angle region.

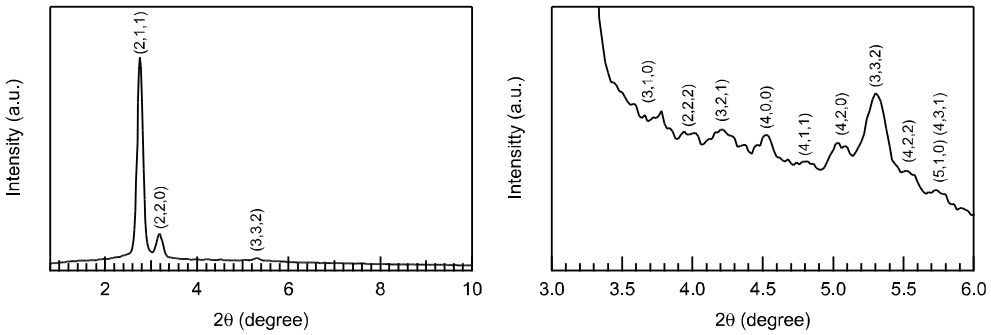

Figure S6 X-ray scattering profiles in the small angle region of the cubic phase (140 ^{o}C) observed in the racemic mixture.

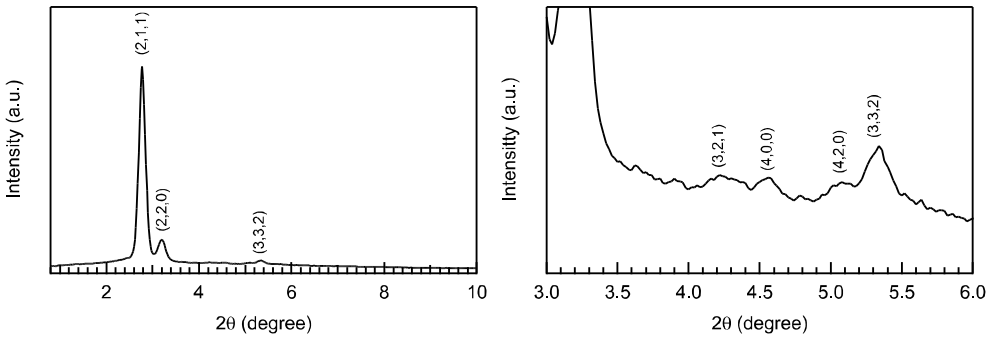

Figure S7 X-ray scattering profiles in the small angle region of the chiral cubic phase (I432) observed in the mixture of (*S*,*S*)-**AZO-PP**/(*R*,*R*)-**AZO-PP** = 35/65 at 105 ^{o}C.

4. DSC study on the racemic mixture

The thermodynamic properties of the racemic mixture are also examined by DSC (figure S8), indicating that the obtained cubic phase is enantiotropically stable between 80 ^{o}C and 176 ^{o}C with the enthalpy changes of 8.3 kJ/mol and 2.8 kJ/mol at the crystal-cubic and cubic-isotropic liquid phase transitions, respectively.

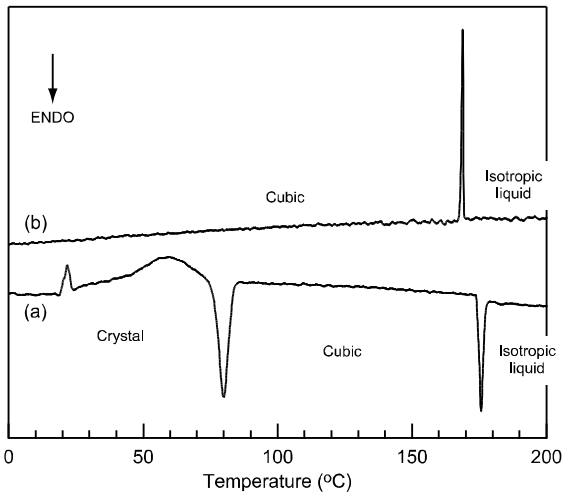

Figure S8 DSC thermograms of the racemic mixture: (a) on heating (+5 ^{o}C min^{-1}) and (b) on cooling (-5 ^{o}C min^{-1}).

5. On the effect of temperature increase during the UV beam irradiation

The increase of temperature during the UV irradiation was experimentally evaluated as follows. We irradiated the focused UV beam (λ = 365 nm, I = 1.5 mW/cm^2) onto a conventional nematic liquid crystal (4-pentyl-4'-cyanobiphenyl) and at the same time we measured the transition temperature of the sample. By the comparison of the transition temperatures between irradiated and non-irradiated conditions, temperature increase by the focused UV beam irradiation was estimated to be *ca*. 0.5 ^{o}C.

During our experiments reported in Figures 4(a) and 4(b), we irradiated the UV beam at the temperature substantially lower than the transition temperatures, i.e., 20 ^{o}C and 4 ^{o}C below the SmQ_L-to-SmQ_H and chiral cubic-to-SmQ_H phase transition temperatures, respectively. Considering that the thermal effect on the temperature increase is within 1 ^{o}C, the photochemical process plays a main role in the induction of the phase transition.

In addition, we recognized the other experimental fact that the hexagonal shape of the irradiated area, in which the induced phase transition occurs, does not change as a function of irradiation time. If the thermal effect caused the phase transition, the photoinduced phase-transition area would be expanded with increasing the irradiation time, resulting in the changes in the shape and size of the phase-transition area. However, in this study, we observed no expansion of phase transition area in the

photoirradiation experiments, suggesting that the *cis* isomers rapidly went back to *trans* isomers outside the irradiated area. On the basis of these experimental results, we believe that the photochemical effect (*cis-trans* photoisomerization) is responsible for the phase transition observed in this study.

Furthermore, the thermal effects have been discussed in the previous report by Ikeda et al.[6], they confirmed that the laser beam did not raise the sample temperature.

References

1 T. Yamamoto, I. Nishiyama and H. Yokoyama, *Chem. Lett*., **2007**, *36*, 1108.

2 T. Yamamoto, I. Nishiyama and H. Yokoyama, *Ferroelectrics*, **2008**, *365*, 39.

3 A.-M. Levelut, E. Hallouin, D. Bennemann, E. Heppke and D. Lötzsch, *J. Phys. II France*, **1997**, *7*, 981.

4 B. Pansu, Y. Nastishin, M. Impéror-Clerc, M. Veber and H. Nguyen, *Eur. Phys. J. E*, **2004**, *15*, 225.

5 H. T. Nguyen, M. Ismaili, N. Isaert and M. F. Achard, *J. Mater. Chem.*, **2004**, *14*, 1560.

6 T. Ikeda and O. Tsutsumi, *Science*, **1995**, *268*, 1873.